Novel combinatorial screening identifies neurotrophic factors for selective classes of motor neurons

Sébastien Schaller[a], Dorothée Buttigieg[a], Alysson Alory[a], Arnaud Jacquier[a], Marc Barad[b], Mark Merchant[c], David Gentien[d], Pierre de la Grange[e], and Georg Haase[a,1]

[a]Institut de Neurosciences de la Timone, UMR 7289 CNRS, Aix-Marseille University, 13005 Marseille, France; [b]Centre d'Immunologie de Marseille-Luminy (CIML), CNRS, INSERM, Aix-Marseille University, 13288 Marseille, France; [c]Genentech Inc., South San Francisco, CA 94080; [d]Institut Curie, Translational Research Department, Genomic Platform, PSL Research University, 75248 Paris, France; and [e]GenoSplice Technology, Institut du Cerveau et de la Moëlle (ICM), Hôpital Pitié Salpêtrière, 75013 Paris, France

Edited by Don W. Cleveland, University of California, San Diego, La Jolla, CA, and approved February 8, 2017 (received for review September 14, 2016)

Numerous neurotrophic factors promote the survival of developing motor neurons but their combinatorial actions remain poorly understood; to address this, we here screened 66 combinations of 12 neurotrophic factors on pure, highly viable, and standardized embryonic mouse motor neurons isolated by a unique FACS technique. We demonstrate potent, strictly additive, survival effects of hepatocyte growth factor (HGF), ciliary neurotrophic factor (CNTF), and Artemin through specific activation of their receptor complexes in distinct subsets of lumbar motor neurons: HGF supports hindlimb motor neurons through c-Met; CNTF supports subsets of axial motor neurons through CNTFRα; and Artemin acts as the first survival factor for parasympathetic preganglionic motor neurons through GFRα3/Syndecan-3 activation. These data show that neurotrophic factors can selectively promote the survival of distinct classes of embryonic motor neurons. Similar studies on postnatal motor neurons may provide a conceptual framework for the combined therapeutic use of neurotrophic factors in degenerative motor neuron diseases such as amyotrophic lateral sclerosis, spinal muscular atrophy, and spinobulbar muscular atrophy.

neurotrophic factor | motor neuron | screening | fluorescence-activated cell sorting | Artemin

According to the neurotrophic theory (1), populations of developing neurons compete during their period of programmed cell death for limiting amounts of target-derived neurotrophic factors (NTFs), which determines their survival or elimination; this is well illustrated in the embryonic chicken spinal cord where motor neurons show increased cell death after limb bud removal and increased survival after transplantation of a supernumerary limb bud (2). More than 15 NTFs belonging to different protein families and activating distinct receptors and signaling pathways have now been identified for developing motor neurons (3, 4); some are also able to rescue degenerating motor neurons in experimental models of motor neuron diseases, such as amyotrophic lateral sclerosis (ALS) (5).

Mounting evidence suggests that NTFs act in a combinatorial manner. Indeed, knockout of individual NTF genes in mice causes only partial motor neuron loss (3), whereas genetic ablation of cell types releasing multiple NTFs, such as Schwann cells (6) or muscle cells (7), causes almost complete motor neuron loss. Similarly, genetic double knockout of the NTFs IGF1 and LIF (8) or triple knockout of CNTF, CT1, and LIF (9) enhances motor neuron loss compared with respective single or double knockouts. NTFs also synergize to rescue motor neurons after axotomy (10) and in culture (11). Finally, combined administration of the NTFs BDNF + CNTF (12) or NT-3 + CNTF (13) reduces pathologic motor neuron degeneration in *wobbler* and *pmn* mice, respectively.

The mechanistic basis for these combinatorial NTF effects remains unclear. One hypothesis postulates the existence of motor neuron subsets with different trophic requirements (3, 4). Testing this hypothesis in a comprehensive manner was hitherto precluded by the plethora of NTFs, the early lethality of many NTF/NTF receptor knockout mouse lines, and the poor characterization of motor neuron subsets in traditional primary cultures of embryonic spinal cord.

To systematically investigate the combinatorial action of NTFs, we screened 66 pairwise combinations of 12 NTFs on pure, highly viable, and perfectly standardized embryonic mouse motor neurons isolated by a unique FACS technique. We demonstrate potent, strictly additive, survival effects of hepatocyte growth factor (HGF), ciliary neurotrophic factor (CNTF), and Artemin (ARTN) due to their selective action on distinct classes of motor neurons.

Results

High-Speed FACS Isolation of Motor Neurons. To generate pure, highly viable, and standardized motor neurons, we here set up a unique FACS technique. Using a Becton Dickinson ARIA II FACS sorter, we isolated motor neurons from lumbar spinal cords of embryonic Hb9:GFP mice (14) and seeded them with the built-in AutoClone system directly at predefined numbers on 24-, 96-, or 384-well culture plates (Fig. 1*A* and *SI Appendix*, Fig. S1*A*).

We show that the FACS-isolated cells are all strongly GFP positive and large sized, in contrast to the heterogeneous cell population before FACS (Fig. 1*B*); they express the motor neuron markers CHAT (100%), SMI 32 (100%), and ISL (95.2 ± 2.4%),

Significance

Neurotrophic factors are endogenous survival factors for developing neurons during their programmed cell death, and represent therapeutic candidates in several neurodegenerative diseases. Studies in the developing spinal cord suggest that neurotrophic factors promote the survival of motor neurons in a combinatorial manner. To better understand this, we systematically assayed pairwise combinations of neurotrophic factors (NTFs) on highly standardized motor neuron cultures prepared by a unique FACS technique. Our data unravel potent additivity of three neurotrophic factors due to their specific survival effects on distinct classes of motor neurons innervating different targets. Further analyses are required to better understand combinatorial NTF effects in adulthood and to define optimized NTF combinations for degenerative motor neuron diseases.

Author contributions: G.H. designed research; S.S., D.B., A.A., A.J., M.B., D.G., and G.H. performed research; M.M. contributed new reagents/analytic tools; S.S., D.B., A.J., D.G., P.d.l.G., and G.H. analyzed data; and G.H. wrote the paper.

The authors declare no conflict of interest.

This article is a PNAS Direct Submission.

Data deposition: The microarray data of FACS-isolated motor neurons reported in this paper have been deposited in the Gene Expression Omnibus (GEO) database, www.ncbi.nlm.nih.gov/geo (accession no. GSE86478).

[1]To whom correspondence should be addressed. Email: georg.haase@univ-amu.fr.

This article contains supporting information online at www.pnas.org/lookup/suppl/doi:10.1073/pnas.1615372114/-/DCSupplemental.

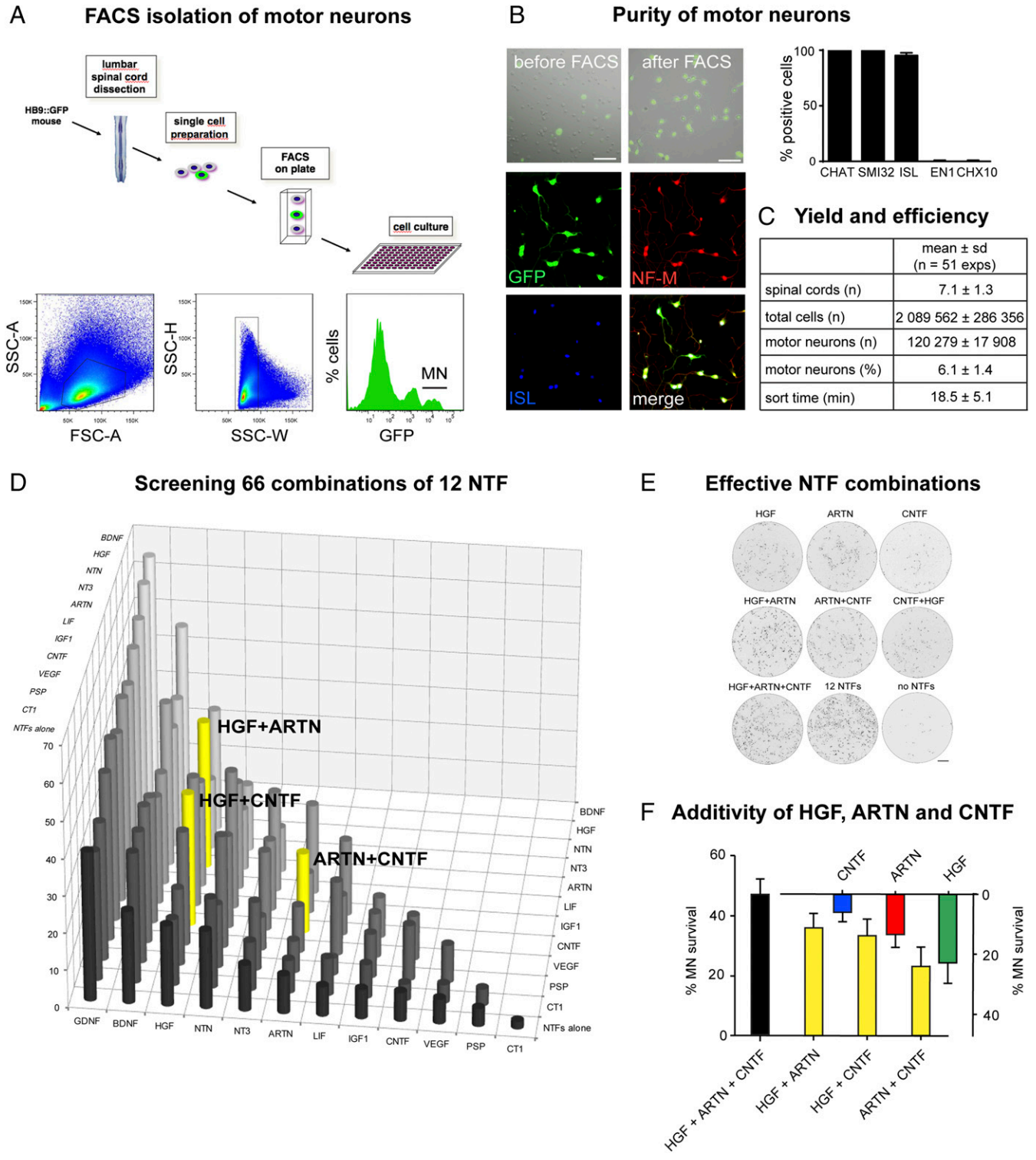

Fig. 1. Screening neurotrophic factor combinations on FACS-isolated motor neurons. (*A*) FACS diagram (*Upper*) depicts FACS-isolation and culture of motor neurons from embryonic E12 Hb9:GFP mice. FACS profiles (*Lower*) show sequential gating of cells through forward-scatter area (FSC-A)/side scatter area (SSC-A), side scatter width (SSC-W)/side scatter height (SSC-H), and GFP fluorescence to isolate motor neurons (MN) (*Right*) from bulk cells (*Left*) and interneurons (*Center*). (*B*) Purity of FACS-isolated motor neurons. GFP/DIC images (*Top*) show cells before and after FACS. 20× objective. (Scale bar: 50 μm.) Immunofluorescence images (*Middle* and *Bottom*) show FACS-isolated motor neurons positive for GFP, neurofilament-M (NF-M), and ISL1/2. The diagram indicates that FACS-isolated cells are positive for motor neuron markers CHAT, SMI32, and ISL1/2 but negative for interneuron markers EN1 and CHX10 (mean ± SD, $n = 4$ replicates). (*C*) Yield and efficiency of FACS-based MN isolation. (*D*) Testing 66 NTF combinations on motor neuron survival reveals potentiated effects of pairwise combinations among HGF, ARTN, and CNTF. $P < 0.0001$ (HGF + CNTF, HGF + ARTN) and $P < 0.04$ (ARTN + CNTF) by Kruskal–Wallis test and Dunn's post hoc test, $n = 12$ wells each, compared with the individual NTFs. Motor neuron survival at 3 DIV is expressed relative to the values for 12 NTFs (100%) and no NTF (0%). (*E*) Whole-well images showing motor neurons cultured for 3 DIV in the presence of the indicated NTFs. (*F*) Diagram showing strictly additive survival effects of HGF, ARTN, and CNTF in pairwise and triple combination (mean ± SD). Statistical significance was tested by Kruskal–Wallis test and Dunn's post hoc test.

but not the interneuron markers EN1 or CHX10 (Fig. 1*B*), and thus represent bona fide motor neurons of exquisite purity.

On a routine basis, we obtain ~120,000 lumbar motor neurons per typical mouse litter within less than 90 min, including <20 min high-speed FACS at maximum flow rate (Fig. 1*C* and *SI Appendix*, Fig. S1*B*). The FACS-isolated motor neurons survive and grow well and in a highly reproducible manner in culture despite the rapid cell acceleration/deceleration and the strong electromagnetic fields encountered during FACS (Fig. 1*B* and *SI Appendix*, Fig. S1 *A* and *B*). These data attest the high yield, rapidity, and standardization of this technique.

Combinatorial Screening of Neurotrophic Factors. To study the combinatorial effects of NTFs, we selected 12 commercially available NTFs belonging to different protein families, including the neurotrophins BDNF and NT3; the GDNF family members GDNF, Neurturin (NTN), ARTN, and Persephin (PSPN); and the cytokines CNTF, CT1, and LIF, as well as HGF, IGF1, and VEGF (3).

We first verified that all NTFs were fully biologically active by comparing side-by-side batches from different suppliers (*SI Appendix*, Fig. S2*A*). Each NTF was tested at its reported optimal concentration in chemically defined medium. FACS-isolated lumbar motor neurons were directly seeded into 96-well plates and their survival assessed by automated imaging analysis. Under these conditions, all NTFs significantly enhanced motor neuron survival. BDNF and GDNF were most effective, whereas PSPN, IGF1, and VEGF were least effective (*SI Appendix*, Fig. S2*A*). For each NTF, there was little variation between batches from different commercial suppliers, suggesting full biological activity of all NTFs (*SI Appendix*, Fig. S2*A*).

In mouse lumbar spinal cord, motor neurons undergo programmed cell death (PCD) between embryonic days E12.5 and E14.5 (15). To assay combinatorial NTF effects on lumbar motor neuron PCD, we isolated them before their PCD at E12, seeded them at a low density of 1,000 cells per well, and monitored their survival over 3 d in vitro (DIV). In the absence of any NTFs, the cultured motor neurons died very rapidly (*SI Appendix*, Fig. S2*B*); by contrast, they survived at a high rate in the presence of all NTFs, suggesting potentiation between some NTFs.

To screen the effects of the 66 pairwise NTF combinations, we designed a strict flowchart for experimentation and data analysis (*SI Appendix*, Fig. S3 *A* and *B*) (16). Three pairwise combinations of NTFs turned out to significantly potentiate motor neuron survival (mean ± SD): HGF + ARTN (40 ± 5%), HGF + CNTF (36 ± 6%), and CNTF + ARTN (22 ± 6%), in comparison with HGF (22 ± 7%), ARTN (10 ± 4%), and CNTF (8 ± 3%), all 12 NTFs (set 100%) or no NTFs (set 0%) (Fig. 1 *D* and *E* and *SI Appendix*, Fig. S3 *C–E*). Interestingly, no such potentiation was seen for HGF, ARTN, or CNTF in combination with the other nine factors (Fig. 1*D* and *SI Appendix*, Fig. S3 *C–E*).

We then found that the triple combination of HGF + ARTN + CNTF is even more effective than the three pairwise combinations and keeps alive 46 ± 5% of motor neurons (Fig. 1 *E* and *F*). Strikingly, this percentage is equivalent to the numerical sum of the effects by the three individual factors (Fig. 1*F*); it is also equivalent to the sum of the effects by one factor and the two others combined (Fig. 1*F*). These data indicate that HGF, ARTN, and CNTF act in a strictly additive manner, suggesting their action on distinct subsets of motor neurons.

Motor Neuron Subsets in Lumbar Spinal Cord. The lumbar spinal cord contains three major subsets of motor neurons that differ in their position, targets, and molecular markers (Fig. 2*A*) (17). Motor neurons of the medial motor column (MMC-MN) innervate axial body muscles and express the transcription factors OCT-6/SCIP-1 and LHX3 (MMCm). Motor neurons of the lateral motor column (LMC-MN) innervate hindlimb muscles and

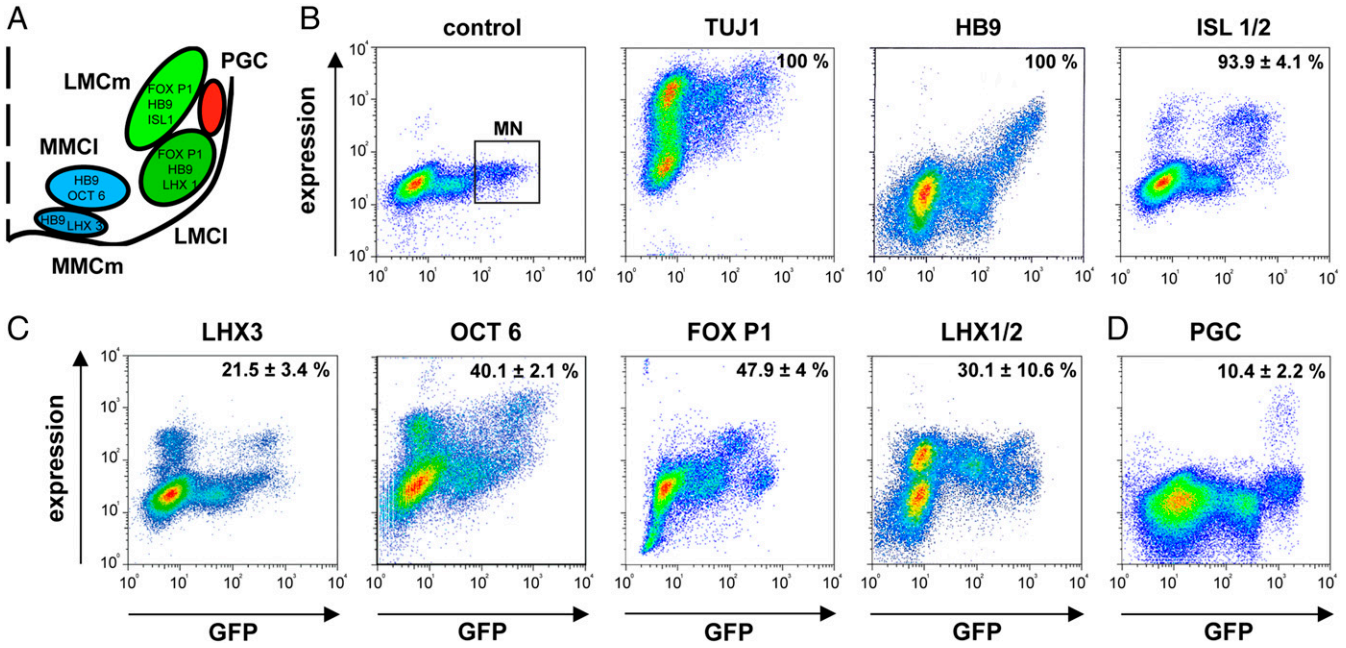

Fig. 2. Quantitation of motor neuron subsets by double-color flow cytometry. (*A*) Schematic depicting position and molecular markers of motor neuron subsets in mouse E12 lumbar spinal cord. (*B*) Density plots indicating the percentage of neurons (TUJ1) and motor neurons (HB9, ISL1/2) in lumbar ventral spinal cord of HB9:GFP mice analyzed by double-color flow cytometry. A representative control (*Left*) showing labeling with isotype-matched primary antibody and indicating the motor neuron population (MN). (*C*) Density plots indicating the percentage of MMC motor neurons (LHX3, OCT6) and LMC motor neurons (FOXP1, LHX1/2) among motor neurons. Note overlap of some markers in motor neuron subsets and expression of LHX3, OCT6, and LHX1/2 in subsets of interneurons. (*D*) Density plot indicating percentage of preganglionic (PGC) neurons after bulk retrograde labeling with tetramethylrhodamine-dextran from bladder. Percentages represent means ± SD of 3–4 independent experiments.

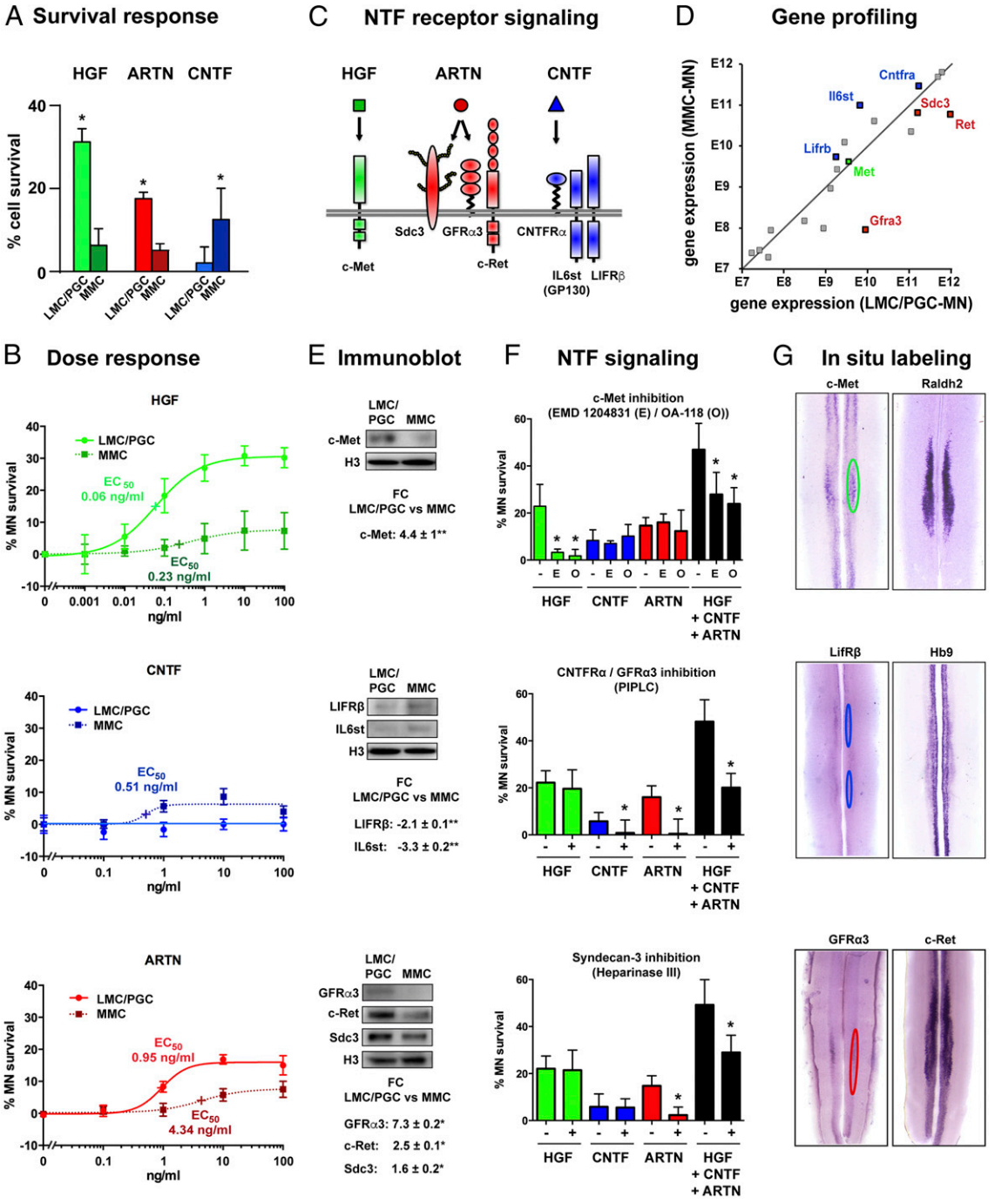

Fig. 3. Characterization of motor neurons responsive to HGF, CNTF, and ARTN. (*A*) Distinct survival responses of LMC/PGC-MN and MMC-MN to HGF, ARTN, and CNTF (mean ± SD, $*P < 0.05$, Mann–Whitney test). (*B*) Dose–response curves. Semimaximal effective concentrations (EC_{50}) of HGF and ARTN are 3.8× and 4.5× lower, respectively, for LMC/PGC-MN than for MMC-MN. EC_{50} 95% confidence intervals do not overlap (not shown). (*C*) Schematic showing HGF, ARTN, and CNTF receptor complexes. (*D*) Gene expression profiling of MN subsets. Note up-regulation of Lifrb (1.4-fold, $P < 0.03$) and Il6st/Gp130 (2.3-fold, $P < 0.0003$) in MMC-MN and of Gfra3 (fourfold, $P < 0.0006$), Ret (2.3-fold, $P < 0.0003$), and Sdc3 (1.3-fold, $P < 0.008$) in LMC/PGC-MN. No differential gene expression was seen for Met (in gray) and the receptors of the nine other NTFs (in gray). Student's *t* test, $n = 3$ independent sample pairs. (*E*) Immunoblot showing differential expression (FC, fold change) of HGF, CNTF, and ARTN receptor components in LMC/PGC-MN vs. MMC-MN. Histone H3 indicates equal loading. $**P < 0.0003$, $*P < 0.03$, Mann–Whitney test, $n = 4$ independent blots each. (*F*) NTF signaling. Inhibition of c-Met (*Top*) with the c-Met kinase inhibitor EMD 1204831 (E, 100 nM) reduces survival of HGF-responsive MN by 21% and of HGF + CNTF + ARTN responsive MN by 19%. The c-Met neutralizing antibody OA-118 (O, 0.5 μg/mL) has similar effects. Inhibition of CNTFRα and GFRα3 signaling (*Middle*) with PIPLC specifically blocks the effects of CNTF and ARTN. Inhibition of the ARTN coreceptor Sdc3 (*Bottom*) with Heparinase III specifically affects survival of ARTN-responsive MN. Mean ± SD, six wells per condition. *Kruskal–Wallis and Dunn's post hoc test. Cell survival is expressed relative to values for all NTFs (100%) or no NTF (0%). (*G*) In situ labeling in E12 lumbar spinal cord. c-Met–positive MN (*Top*) are located in the LMC labeled by Raldh2. Lifrβ-positive MN (*Middle*) are located in the MMC identified by strong Hb9 mRNA expression. Gfrα3-positive MN (*Bottom*) are positioned in the lower lumbar and sacral spinal cord and represent a fraction of c-Ret-positive neurons.

express FOX P1 and LHX 1/2 (LMCl) (18). Preganglionic motor neurons (PGC-MN) of the sympathetic and parasympathetic nervous system ensure the innervation of ganglionic neurons in pelvic organs and express nNOS, HNF-6, and low levels of FOX P1 (19).

Before testing the potentially distinct effects of HGF, ARTN, and CNTF on these motor neuron subsets, we verified their percentages in the FACS single-cell suspensions. Double-color flow cytometry analysis confirmed that all GFP-positive motor neurons express the generic MN markers HB9 (100%) and ISL 1/2 (94 ± 4%, mean ± SD) (Fig. 2*B*), and 40 ± 2% of them express the MMC marker OCT 6 and 22 ± 3% the MMCm marker LHX3 (Fig. 2*C*), in line with the fraction of LHX3/HB9 MN in mouse spinal cord (20). However, 30.1 ± 10.6 are positive for the LMCl marker LHX1/2, and 48 ± 4% for the LMC/PGC marker FOX P1 (Fig. 2*C*).

Because reported PGC-specific antibodies were not suitable for flow cytometry, we identified PGC-MN by bulk retrograde labeling from bladder using fluorescent tetramethylrhodamine-dextran, yielding ∼10 ± 2% labeled cells (Fig. 2*D*), in keeping with the 1:4 ratio of lumbar PGC-MN to LMC-MN (18).

These data demonstrate that LMC-MN, MMC-MN, and PGC-MN are present in single-cell FACS preparations at similar percentages as in vivo, warranting analysis of their responses to neurotrophic factors.

Distinct Effects of HGF, CNTF, and ARTN on Motor Neuron Subsets. There are currently no established methods to specifically isolate and culture MMC-MN, LMC-MN, or PGC-MN from rodents. To overcome this issue, we isolated lumbar MMC-MN from LMC-MN and PGC-MN by anatomic dissection and FACS (*Experimental Procedures*). Using gene expression profiling on microarrays, we demonstrated that MMC-MN show strong up-regulation of the MMC markers Lhx3, Lhx4, and Oct6/Pou3f1, whereas LMC/PGC-MN show strong up-regulation of the LMC markers Raldh2 and Lhx1, and the PGC markers Nos1 (nNos), Hnf6, and Smad1 (*SI Appendix*, Fig. S4*A*). Global gene expression profiles were highly correlated between independent replicate samples (MMC-MN: $R = 0.9924$; LMC/PGC-MN: $R = 0.9899$; *SI Appendix*, Fig. S4*B*). We further verified that in culture, MMC-MN and LMC/PGC-MN have a similar survival rate in the presence of all 12 NTFs and undergo rapid indistinguishable cell death in the absence of any NTF (*SI Appendix*, Fig. S5*A*).

The strong enrichment, high standardization, and similar global survival response of FACS-isolated MMC-MN and LMC/PGC-MN enabled us to compare the effects of individual NTFs. We found that HGF and ARTN support the survival of a large fraction of LMC/PGC-MN (HGF: 30 ± 3%; ARTN: 17 ± 1%) but have a minor effect on MNC-MN (Fig. 3*A*). By contrast, CNTF supports the survival of 12 ± 7% of MMC-MN but has no effect on LMC/PGC-MN (Fig. 3*A*). These differential effects of HGF, CNTF, and ARTN were confirmed by dose–response curves showing significant differences in their semimaximal effective concentrations (EC_{50}) for each MN subset (Fig. 3*B*). No differential effects were seen with the other nine NTFs (*SI Appendix*, Fig. S5*B*). HGF and ARTN thus preferentially promote the survival of LMC/PGC-MN, whereas CNTF selectively promotes the survival of MMC-MN.

Differential Expression of the HGF, CNTF, and ARTN Receptors in Motor Neuron Subsets. The differential survival response of LMC/PGC-MN vs. MMC-MN to HGF, ARTN, and CNTF prompted us to analyze their expression of NTF receptors (Fig. 3*C*) by microarray and Western blot analyses.

HGF is known to trigger survival through the transmembrane receptor c-Met (Fig. 3*C*). We found that c-Met is not differentially regulated at the mRNA level (Fig. 3*D*) but increased by 4.4 ± 0.54-fold (mean ± SD) at the protein level in LMC/PGC-MN compared with MMC-MN (Fig. 3*E*, *Top*), in agreement with the preferential response of LMC/PGC-MN to HGF.

The CNTF receptor comprises the CNTFRα receptor and the two signal-transducing components LIFRβ and IL6st (GP130) (Fig. 3*C*). LIFRβ and GP130 are significantly up-regulated in MMC-MN both at the mRNA (Fig. 3*D*) and the protein level (Fig. 3*E*, *Middle*), in line with the specific response of MMC-MN to CNTF (Fig. 3 *A* and *B*). Interestingly, CNTFRα is not differentially regulated, potentially reflecting the presence of soluble forms signaling in trans (21).

ARTN signals through a receptor complex composed by GFRα3, the proteoglycan coreceptor Syndecan-3 (Sdc3), and the signal transducing tyrosine kinase c-Ret (Fig. 3*C*). We found that GFRα3, Sdc3, and c-Ret are all strongly up-regulated in LMC/PGC-MN at the mRNA (Fig. 3*D*) and the protein level (Fig. 3*E*, *Bottom*), which matches the preferential response of LMC/PGC-MN to ARTN. No such differential regulation was seen for the receptors of the other NTFs tested (Fig. 3*D*).

HGF/c-Met Signaling Promotes Survival of Limb-Innervating LMC Motor Neurons. To characterize the motor neuron subsets supported by HGF, ARTN, and CNTF, we used specific inhibitors to block NTF receptor-mediated survival signaling in culture (Fig. 3*F*) and analyzed the expression of the corresponding NTF receptors in E12 lumbar spinal cord (Fig. 3*G*).

To analyze HGF/c-Met survival signaling in lumbar motor neurons, we used EMD 1204831, a c-Met tyrosine kinase inhibitor with minimal off-target effects (22). We found that EMD 1204831 (100 nM) completely abrogates the survival effects of HGF and partially those of HGF + ARTN + CNTF but not those of ARTN or CNTF alone (Fig. 3*F*, *Top*). Similar effects were seen with OA-118, a monovalent antibody that neutralizes c-Met signaling (Fig. 3*F*, *Top* and *SI Appendix*, *Supplemental Material and Methods*).

To localize the HGF-responsive lumbar motor neurons, we performed whole-mount in situ hybridizations and detected the c-Met positive motor neurons almost exclusively in the LMC identified by the LMC marker Raldh2 (Fig. 3*G*, *Top*). The c-Met–positive MN form well-delineated groups potentially corresponding to individual motor pools innervating limb muscles (Fig. 3*G*, *Top*). Few c-Met–positive motor neurons are also present in the adjacent thoracic and sacral spinal cord, in line with an earlier report (23). Taken together, these data indicate that HGF specifically promotes the survival of a fraction of hindlimb-innervating LMC motor neurons through activation of the c-Met tyrosine kinase receptor.

CNTF/CNTFRα Signaling Supports Subsets of Axial Muscle-Innervating MMC Motor Neurons. We then blocked CNTF signaling by using phosphoinositol phospholipase C (PIPLC), an enzyme that cleaves the phosphoinositol side chain of the CNTFRα receptor necessary for its plasma membrane insertion (24); this completely blocks the survival of CNTF-dependent motor neurons but has no effect on the survival of HGF-dependent motor neurons (Fig. 3*F*, *Middle*).

We localized the CNTF-responsive motor neurons by whole-mount in situ hybridization of Lifrβ (Fig. 3*G*, *Middle*), which revealed two distinct small MN subsets in the MMC identified by strong Hb9 mRNA expression. We conclude that CNTF specifically promotes the survival of two MMC-MN subsets by activating survival signaling triggered by CNTFRα and, presumably, LIFRβ/GP130.

ARTN Acts as a Survival Factor for Parasympathetic Preganglionic Motor Neurons Through GFRα3/Sdc3 Signaling. ARTN has not been previously recognized as a neurotrophic factor for motor neurons. To analyze ARTN survival signaling, we used Heparinase III, which cleaves the proteoglycan side chains of the ARTN coreceptor Sdc3 (25). We show that Heparinase III almost completely blocks the survival of motor neurons depending on ARTN (Fig. 3*F*,

Bottom). Similar effects were seen with PIPLC (Fig. 3*F*, *Middle*), which cleaves the phosphoinositol chain of GFRα3 (26), and with antibodies against the extracellular domain of GFRα3 (*SI Appendix*, Fig. S6). ARTN-mediated survival effects were not inhibited with neutralizing antibodies against GFRα1 (*SI Appendix*, Fig. S6), the preferred α-receptor of GDNF (26), indicating specificity.

To localize the ARTN-responsive motor neurons, we performed whole-mount immunolabeling, demonstrating that GFRα3-positive cells represent a fraction of c-Ret–positive cells (Fig. 3*G*, *Bottom*). The GFRα3-positive cells are localized in a tiny column that extends from lumbar L5 to sacral S2 segments (Fig. 3*G*, *Bottom*) at a lateral spinal cord position (Fig. 4*A*) reminiscent of parasympathetic preganglionic (PGC) motor neurons innervating urogenital sphincter organs; to confirm this, we demonstrated that GFRα3-positive cells coexpress the PGC marker nNOS (Fig. 4*B*) and fluorescent dextrans retrogradely bulk injected into bladder (Fig. 4*C*). As expected for an NTF receptor, GFRα3 is expressed in PGC cell bodies (Fig. 4*D*) and ventral root axons labeled by neurofilament M (Fig. 4*A*).

Taken together, these data identify ARTN as a survival factor for parasympathetic preganglionic motor neurons through activation of GFRα3/Sdc3 signaling.

Discussion

In sum, using a combinatorial screening on highly standardized motor neuron cultures, we here identify previously unrecognized survival effects of the three neurotrophic factors HGF, CNTF, and ARTN on distinct subsets of motor neurons in the lumbar spinal cord.

We demonstrate that HGF almost exclusively supports hindlimb-innervating LMC motor neurons through activation of c-Met kinase (Fig. 3 *D–F*). Remarkably, the strong up-regulation of the receptor c-Met in hindlimb motor neurons (Fig. 3*G*) perfectly matches the restricted expression of its ligand HGF in its target muscles in the limb (27, 28), which nicely illustrates the neurotrophic theory. The effects of HGF on limb-innervating motor neurons may also underlie its strong therapeutic potency in mutant SOD1 ALS model mice, where it reduces limb muscle paralysis and increases limb muscle weight (29).

The specific action of CNTF on subsets of axial MMC-MN was more surprising but is in line with its reported potent effects on MMC-MN in spinal cord slice cultures (ref. 30, figure 8) and its weak effects on axotomized neonatal LMC-MN (10). According to our data, the CNTF-responsive MMC motor neurons represent less than 10% of total at embryonic stage E12 (Figs. 1*D* and 3 *A* and *B*). This finding contrasts with the massive loss of motor neurons (33–40%) in knockout mice for the CNTF receptor genes Lifrb, gp130, or Cntfra around birth (3), suggesting additional roles for CNTF or CNTF-like cytokines during late embryonic development.

ARTN has been previously shown to support peripheral sympathetic neurons (26, 31). We here identify ARTN as a survival factor for parasympathetic preganglionic motor neurons in the lumbosacral spinal cord (Fig. 4 *A–D*), which connect to ganglionic neurons in distal colon, bladder, and genital sphincter organs (32, 33).

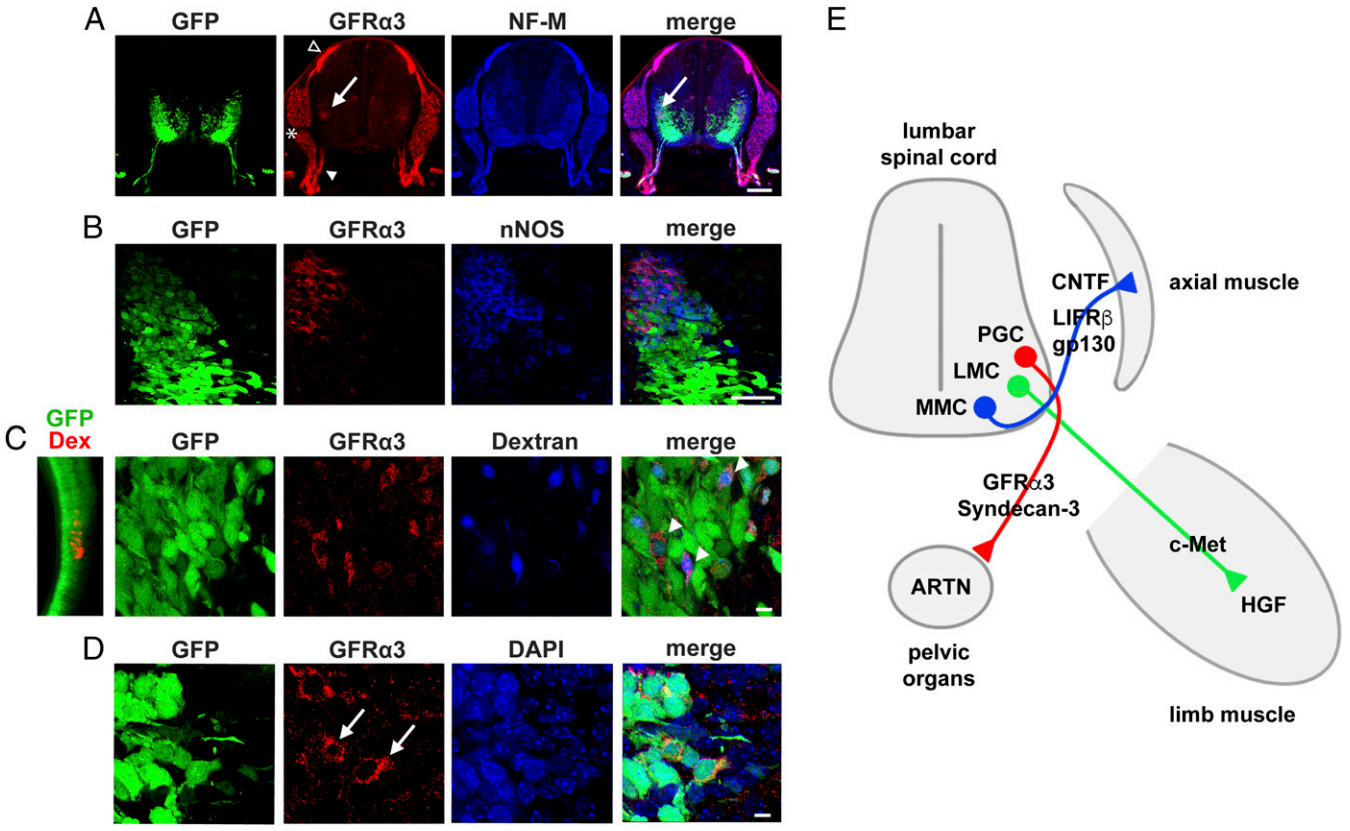

Fig. 4. GFRα3 expression in parasympathetic preganglionic motor neurons. (*A*) Overview images showing position of GFRα3-positive motor neurons colabeled for NF-M in lower lumbar spinal cord of E12 Hb9:GFP mice. Cell bodies are indicated by arrow and ventral root axons by filled arrowhead. GFRα3 is also strongly expressed in some DRG neurons (asterisk) and the dorsal root entry zone (open arrowhead). (*B*) Images showing GFRα3 expression in PGC motor neurons identified by nNOS. (*C*) (*Left*) Lumbosacral spinal cord after retrograde bulk labeling with tetramethylrhodamine-dextran from developing bladder. (*Right*) GFRα3-positive cells retrogradely labeled from bladder with Alexa 647-dextran (arrowheads in merge). (*D*) GFRα3 expression in cell bodies of PGC motor neurons (arrows). Nuclei are labeled with DAPI. (Scale bars: *A*, 100 μm; *B*, 50 μm; *C* and *D*, 10 μm.) (*E*) Schematic indicating a close match between the expression of NTF receptors in lumbar LMC, MMC, and parasympathetic PGC motor neurons and the expression of the NTF ligands in the corresponding target tissues and organs.

Consistent with this novel role, ARTN is expressed in these target organs (34); its receptor GFRα3 is expressed in the axons and cell bodies of PGC-MN during development (Fig. 4 *A* and *D*) and adulthood (33); and transgenic ARTN causes hyperplasia of parasympathetic nerves (34).

Our findings on HGF, CNTF, and ARTN leave open potential combinatorial effects of other NTFs. Indeed, several NTF combinations, including BDNF + GDNF, tended to be effective in our screen without, however, reaching statistical significance (*SI Appendix*, Fig. S3 *C–E*). Furthermore, all NTFs were assayed here at their reported optimal concentration, which favors additive rather than synergistic effects. This may explain why GDNF + CT1, which synergize on motor neurons at low concentration (11), failed to do so at high concentration (*SI Appendix*, Fig. S3 *C–E*). Similarly, the design of our screen may have missed the detection of sequential NTF effects—in particular, of NTFs with short half-lives, because NTFs were only added once at the start of the cultures. Finally, several of the NTFs tested here not only promote motor neuron survival but also favor axon and dendrite growth as well as synapse formation (3, 4). These considerations warrant further analyses on combinatorial NTF effects in developing motor neurons.

Are screens on cultured motor neurons to some extent predictive for clinical trials in human motor neuron disease? Published studies with small molecule compounds provide first hints. Indeed, both Olesoxime (TRO19622) (35) and Kenpaullone (36) have been identified in survival screens on neurotrophic factor-deprived motor neurons. Olesoxime, a cholesterol-like molecule, showed positive effects in human spinal muscular atrophy (SMA) (37) but was ineffective in ALS (38). Kenpaullone, an inhibitor of the phospho c-Jun–mediated apoptotic pathway, was reported to be effective on motor neurons carrying mutations in the human ALS genes SOD1 (36) or FUS (39).

Most NTFs have failed in past clinical trials (40), and this failure was widely attributed to delivery problems of the recombinant proteins. In preclinical ALS and SMA models, however, several NTFs have provided substantial therapeutic benefit when delivered by gene- or cell-based systems (13, 41, 42). Importantly, a meta-analysis of 226 studies in mutant SOD1 mice (5) has identified four NTFs among the six most-effective treatments (apart from SOD1 modifiers), which prolonged the animal's survival by >30%.

It should however be stressed that the response of postnatal motor neurons to NTFs is largely unknown and potentially differs from that of developing motor neurons (our study). Ongoing research efforts thus aim to isolate disease-relevant motor neuron subsets at a postnatal stage to determine their NTF receptor profile and to compare their survival response to NTFs (43, 44). These types of studies may help to tailor future experimental NTF therapies to those motor neurons that are preferentially affected in each form of motor neuron disease, i.e., limb-innervating motor neurons in classical ALS, proximal motor neurons in SMA, and brainstem motor neurons in bulbar ALS or spinobulbar muscular atrophy (4, 45).

Experimental Procedures

Mice. Transgenic Hb9:GFP mice [line mHB9-Gfp1b (14), kindly provided by T. Jessell] were maintained on a C57/BL6 background and mated with female CD1 mice (Charles River). All experiments with mice were performed in strict compliance with institutional and national guidelines and approved by Marseille's Ethics Committee No. 71.

FACS and Cell Culture. Lumbar spinal cords were dissected from E12 Hb9:GFP embryos, and longitudinal ventral spinal cord segments Th13 to S1 isolated under a Leica MZ16FA fluorescence stereomicroscope. Single-cell suspensions were prepared as described (46), resuspended in a 1:1 (vol/vol) mix of L15 medium:Facsflow, and subjected to FACS with an ARIA II SORP (Becton Dickinson). Cells were isolated at a sheath pressure of 45 pounds/psi through an 85-μm nozzle, seeded with the AutoClone system in culture wells coated with polyornithin/laminin, and cultured in supplemented Neurobasal medium without riboflavin.

Screening NTF Combinations. Effects of pairwise NTF combinations were assayed in a two-step test/retest procedure (*SI Appendix*, Fig. S3 *A* and *B*). Survival of calcein-positive motor neurons was assessed by imaging entire wells with an inverted microscope (DMI 4000B, Leica, 1.25× objective, DX360 camera). Images were processed with ImageJ software and analyzed by an experimenter masked to the experimental conditions.

Flow Cytometry. Single-cell suspensions were taken up in DMEM/F12, fixed for 15 min on ice in 2% (wt/vol) formaldehyde in PBS, washed twice in PBS 0.1% BSA, and permeabilized for 15 min on ice in PBS 0.5% saponin (wt/vol). Flow cytometry was performed essentially as described (47). Cell suspensions were incubated overnight at 4 °C with primary antibodies against Hb9, Isl 1/2, Lhx 1/2, Lhx3, Foxp1, Oct6 (*SI Appendix*, Table 2) or with control antibodies, washed twice, and incubated for 45 min at 4 °C with secondary antibodies. After two washes, cells were resuspended in PBS 1% BSA, analyzed with a FACS ARIA II SORP or a FACS ARIA III and data plotted with FlowJo software (Tree Star).

Statistical Analyses. Each experiment was performed with several biological replicates (see figure legends) and repeated at least twice. Data were analyzed with GraphPad Prism 6 (GraphPad). Data from two groups showing Gaussian distribution were analyzed with Student's *t* test two-tailed; otherwise, the Mann–Whitney test was used. Data from more than two groups were analyzed with the Kruskal–Wallis test and Dunn post hoc test. Dose–response curves, EC_{50} values, and 95% confidence intervals were computed using a nonlinear fit model with variable slope. Cytometry data were tested for significance with the χ^2 test using FlowJo software.

SI Appendix provides experimental details on gene expression profiling, immunoblot analyses, whole-mount labeling, immunohistochemistry, retrograde labeling, and signaling studies.

ACKNOWLEDGMENTS. We acknowledge the contribution of A. Gonté and E. Buhler as well as Drs. D. Bohl and S. Blanchard to an early stage of this work. We thank Drs. F. Tell for expert advice on statistical data analysis; S. Zaffran for logistic help with in situ hybridization; Prof. Michael Schaefer for expert help with gene expression analyses; Drs. P. Zimmermann, S. Driegen, and F. Clotman for providing antibodies; F. Bladt for providing the c-Met tyrosine kinase inhibitor EMD 1204831; Drs. F. Morel and J. L. Boisneault for continuous support; Drs. G. P. Schiavo and C. Rabouille for critical reading of the manuscript; and the reviewers for their incisive comments. This study was financed by grants from Association Française contre les Myopathies (AFM), Agence Nationale pour la Recherche (ANR), ERANET Neuron, INSERM, and Aix-Marseille University. S.S. received salary support from ANR; D.B. received a PhD fellowship from Fondation pour la Recherche Médicale (FRM), AFM, and ANR; A.A. received salary support from ANR; and A.J. was supported by PhD fellowships from INSERM/Région Provence Alpes Côtes d'Azur and FRM.

1. Purves D (1986) *Body and Brain: A Trophic Theory of Neural Development* (Harvard Univ Press, Cambridge, MA).
2. Hamburger V (1977) The developmental history of the motor neuron. The F.O. Schmitt lecture in neuroscience. *Neurosci Res Program Bull* 15(Suppl.):1–37.
3. Gould TW, Enomoto H (2009) Neurotrophic modulation of motor neuron development. *Neuroscientist* 15(1):105–116.
4. Kanning KC, Kaplan A, Henderson CE (2010) Motor neuron diversity in development and disease. *Annu Rev Neurosci* 33:409–440.
5. Turner BJ, Talbot K (2008) Transgenics, toxicity and therapeutics in rodent models of mutant SOD1-mediated familial ALS. *Prog Neurobiol* 85(1):94–134.
6. Riethmacher D, et al. (1997) Severe neuropathies in mice with targeted mutations in the ErbB3 receptor. *Nature* 389(6652):725–730.
7. Grieshammer U, Lewandoski M, Prevette D, Oppenheim RW, Martin GR (1998) Muscle-specific cell ablation conditional upon Cre-mediated DNA recombination in transgenic mice leads to massive spinal and cranial motoneuron loss. *Dev Biol* 197(2):234–247.
8. Vicario-Abejón C, Fernández-Moreno C, Pichel JG, de Pablo F (2004) Mice lacking IGF-I and LIF have motoneuron deficits in brain stem nuclei. *Neuroreport* 15(18):2769–2772.
9. Holtmann B, et al. (2005) Triple knock-out of CNTF, LIF, and CT-1 defines cooperative and distinct roles of these neurotrophic factors for motoneuron maintenance and function. *J Neurosci* 25(7):1778–1787.
10. Vejsada R, Sagot Y, Kato AC (1995) Quantitative comparison of the transient rescue effects of neurotrophic factors on axotomized motoneurons in vivo. *Eur J Neurosci* 7(1):108–115.
11. Arce V, et al. (1998) Synergistic effects of Schwann- and muscle-derived factors on motoneuron survival involve GDNF and cardiotrophin-1 (CT-1). *J Neurosci* 18(4):1440–1448.

12. Mitsumoto H, et al. (1994) Arrest of motor neuron disease in wobbler mice cotreated with CNTF and BDNF. *Science* 265(5175):1107–1110.
13. Haase G, et al. (1997) Gene therapy of murine motor neuron disease using adenoviral vectors for neurotrophic factors. *Nat Med* 3(4):429–436.
14. Wichterle H, Lieberam I, Porter JA, Jessell TM (2002) Directed differentiation of embryonic stem cells into motor neurons. *Cell* 110(3):385–397.
15. Yamamoto Y, Henderson CE (1999) Patterns of programmed cell death in populations of developing spinal motoneurons in chicken, mouse, and rat. *Dev Biol* 214(1):60–71.
16. Malo N, Hanley JA, Cerquozzi S, Pelletier J, Nadon R (2006) Statistical practice in high-throughput screening data analysis. *Nat Biotechnol* 24(2):167–175.
17. Dasen JS, Jessell TM (2009) Hox networks and the origins of motor neuron diversity. *Curr Top Dev Biol* 88:169–200.
18. Rousso DL, Gaber ZB, Wellik D, Morrisey EE, Novitch BG (2008) Coordinated actions of the forkhead protein Foxp1 and Hox proteins in the columnar organization of spinal motor neurons. *Neuron* 59(2):226–240.
19. Francius C, Clotman F (2010) Dynamic expression of the Onecut transcription factors HNF-6, OC-2 and OC-3 during spinal motor neuron development. *Neuroscience* 165(1):116–129.
20. Jung H, et al. (2014) Evolving Hox activity profiles govern diversity in locomotor systems. *Dev Cell* 29(2):171–187.
21. Davis S, et al. (1993) Released form of CNTF receptor alpha component as a soluble mediator of CNTF responses. *Science* 259(5102):1736–1739.
22. Bladt F, et al. (2013) EMD 1214063 and EMD 1204831 constitute a new class of potent and highly selective c-Met inhibitors. *Clin Cancer Res* 19(11):2941–2951.
23. Yamamoto Y, et al. (1997) Hepatocyte growth factor (HGF/SF) is a muscle-derived survival factor for a subpopulation of embryonic motoneurons. *Development* 124(15): 2903–2913.
24. Davis S, et al. (1991) The receptor for ciliary neurotrophic factor. *Science* 253(5015): 59–63.
25. Bespalov MM, et al. (2011) Heparan sulfate proteoglycan Syndecan-3 is a novel receptor for GDNF, Neurturin, and Artemin. *J Cell Biol* 192(1):153–169.
26. Baloh RH, et al. (1998) Artemin, a novel member of the GDNF ligand family, supports peripheral and central neurons and signals through the GFRalpha3-RET receptor complex. *Neuron* 21(6):1291–1302.
27. Ebens A, et al. (1996) Hepatocyte growth factor/scatter factor is an axonal chemoattractant and a neurotrophic factor for spinal motor neurons. *Neuron* 17(6): 1157–1172.
28. Sonnenberg E, Meyer D, Weidner KM, Birchmeier C (1993) Scatter factor/hepatocyte growth factor and its receptor, the c-met tyrosine kinase, can mediate a signal exchange between mesenchyme and epithelia during mouse development. *J Cell Biol* 123(1):223–235.
29. Sun W, Funakoshi H, Nakamura T (2002) Overexpression of HGF retards disease progression and prolongs life span in a transgenic mouse model of ALS. *J Neurosci* 22(15):6537–6548.
30. Rakowicz WP, Staples CS, Milbrandt J, Brunstrom JE, Johnson EM, Jr (2002) Glial cell line-derived neurotrophic factor promotes the survival of early postnatal spinal motor neurons in the lateral and medial motor columns in slice culture. *J Neurosci* 22(10): 3953–3962.
31. Honma Y, et al. (2002) Artemin is a vascular-derived neurotropic factor for developing sympathetic neurons. *Neuron* 35(2):267–282.
32. Park MJ, Chung K (1999) Endogenous lectin (RL-29) expression of the autonomic preganglionic neurons in the rat spinal cord. *Anat Rec* 254(1):53–60.
33. Forrest SL, Payne SC, Keast JR, Osborne PB (2015) Peripheral injury of pelvic visceral sensory nerves alters GFRα (GDNF family receptor alpha) localization in sensory and autonomic pathways of the sacral spinal cord. *Front Neuroanat* 9:43.
34. Bolon B, et al. (2004) The candidate neuroprotective agent Artemin induces autonomic neural dysplasia without preventing peripheral nerve dysfunction. *Toxicol Pathol* 32(3):275–294.
35. Bordet T, et al. (2007) Identification and characterization of cholest-4-en-3-one, oxime (TRO19622), a novel drug candidate for amyotrophic lateral sclerosis. *J Pharmacol Exp Ther* 322(2):709–720.
36. Yang YM, et al. (2013) A small molecule screen in stem-cell-derived motor neurons identifies a kinase inhibitor as a candidate therapeutic for ALS. *Cell Stem Cell* 12(6): 713–726.
37. Finkel R, Bertini E, Muntoni F, Mercuri E (2015) 209th ENMC International Workshop: Outcome Measures and Clinical Trial Readiness in Spinal Muscular Atrophy 7-9 November 2014, Heemskerk, The Netherlands. *Neuromuscul Disord* 25(7):593–602.
38. Lenglet T, et al.; Mitotarget study group (2014) A phase II-III trial of olesoxime in subjects with amyotrophic lateral sclerosis. *Eur J Neurol* 21(3):529–536.
39. Liu ML, Zang T, Zhang CL (2016) Direct lineage reprogramming reveals disease-specific phenotypes of motor neurons from human ALS patients. *Cell Reports* 14(1): 115–128.
40. Gould TW, Oppenheim RW (2011) Motor neuron trophic factors: Therapeutic use in ALS? *Brain Res Brain Res Rev* 67(1-2):1–39.
41. Sendtner M, et al. (1992) Ciliary neurotrophic factor prevents degeneration of motor neurons in mouse mutant progressive motor neuronopathy. *Nature* 358(6386): 502–504.
42. Lesbordes JC, et al. (2003) Therapeutic benefits of cardiotrophin-1 gene transfer in a mouse model of spinal muscular atrophy. *Hum Mol Genet* 12(11):1233–1239.
43. Comley L, et al. (2015) Motor neurons with differential vulnerability to degeneration show distinct protein signatures in health and ALS. *Neuroscience* 291:216–229.
44. Ozdinler PH, Macklis JD (2006) IGF-I specifically enhances axon outgrowth of corticospinal motor neurons. *Nat Neurosci* 9(11):1371–1381.
45. Swinnen B, Robberecht W (2014) The phenotypic variability of amyotrophic lateral sclerosis. *Nat Rev Neurol* 10(11):661–670.
46. Raoul C, et al. (2002) Motoneuron death triggered by a specific pathway downstream of Fas: Potentiation by ALS-linked SOD1 mutations. *Neuron* 35(6):1067–1083.
47. Toli D, et al. (2015) Modeling amyotrophic lateral sclerosis in pure human iPSc-derived motor neurons isolated by a novel FACS double selection technique. *Neurobiol Dis* 82: 269–280.

Novel combinatorial screening identifies neurotrophic factors for selective classes of motor neurons

Sébastien Schaller, Dorothée Buttigieg, Alysson Alory, Arnaud Jacquier, Marc Barad, Mark Merchant, David Gentien, Pierre de la Grange and Georg Haase

Supporting Information (SI) Appendix

Supplemental Fig. S1
Schaller et al.

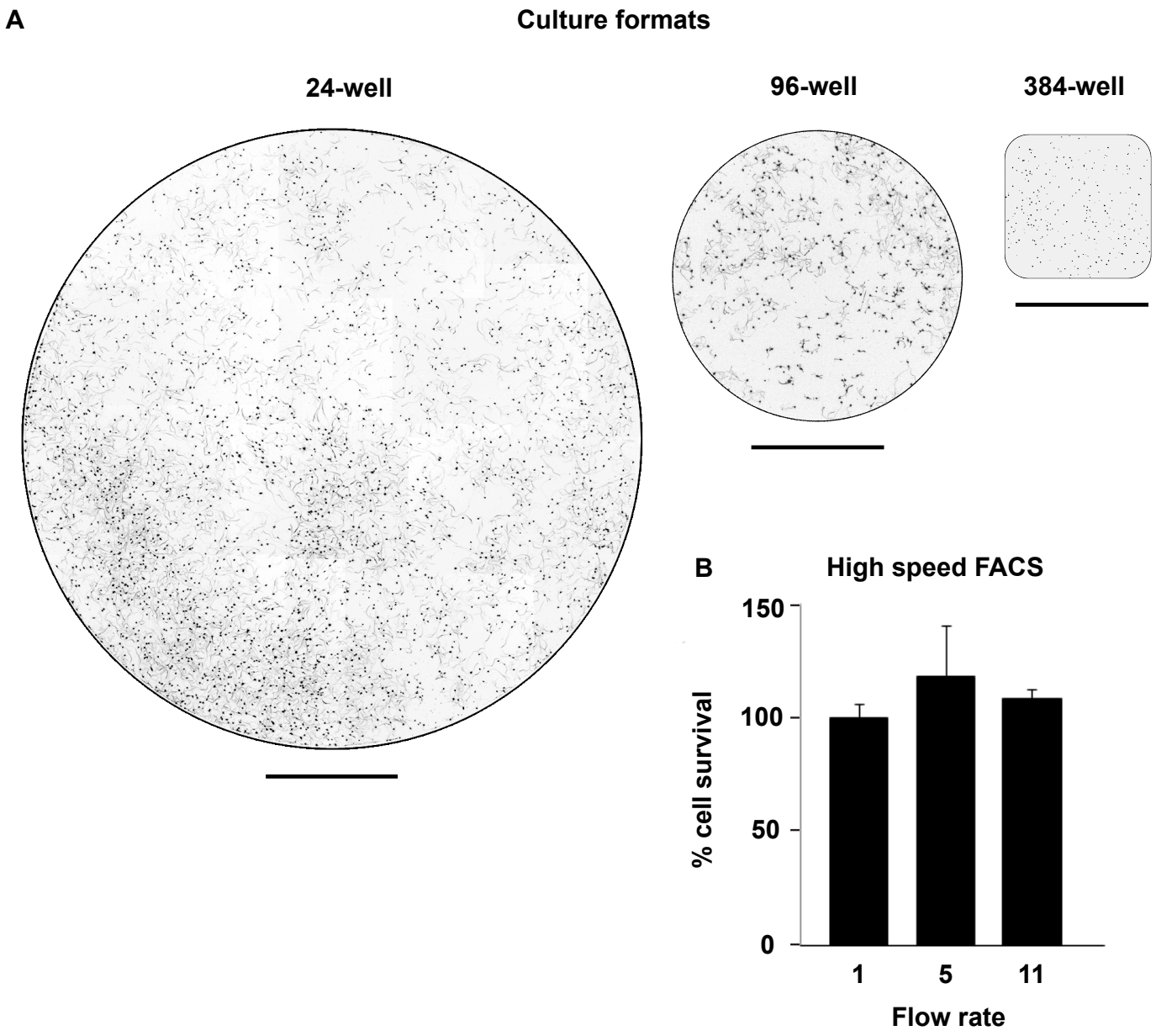

Supplemental Figure S1. High speed FACS-isolation of motor neurons.

A. Images of FACS-isolated motor neurons after 3 DIV culture. Cells are seeded on 24-well plates fitted with 14 mm coverslips (10.000 cells per well), 96-well plates (1.500 cells per well) or 384-well plates (500 cells per well). Scale bar 3 mm.

B. High speed FACS. Motor neurons are isolated at flow rates 1, 5 and 11 corresponding respectively to 14.3, 48.4 and 104 ml/min. Cell survival (mean ± sd) at three days in vitro is indistinguishable after FACS at high flow rate (5, 11) or low flow rate (1). Shown is one out of three representative cultures each done in the presence of 12 NTFs. Differences are not significant by Kruskal Wallis test.

Supplemental Fig. S2
Schaller et al.

A Biological activity of NTFs

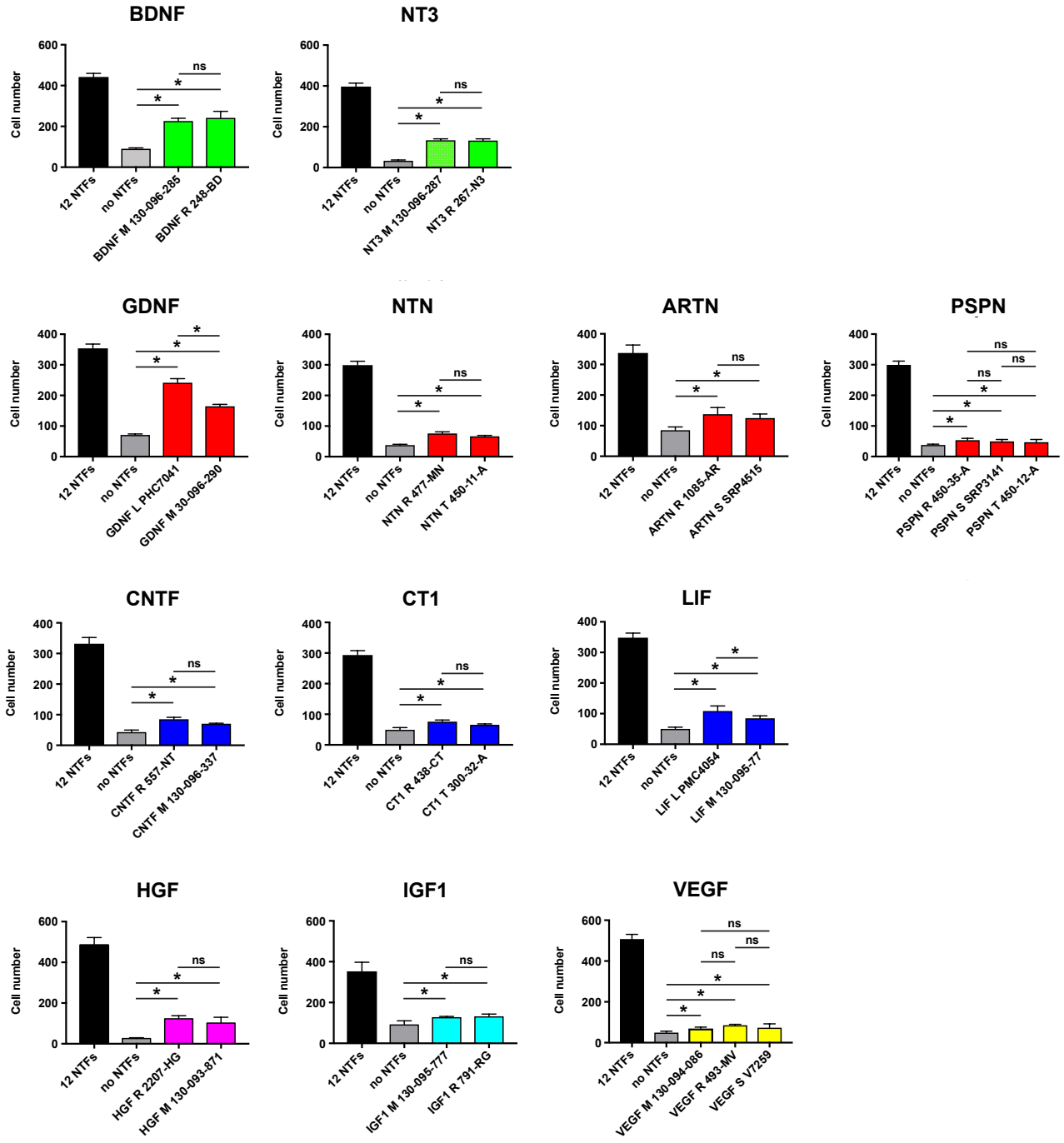

B Survival kinetics of lumbar MNs

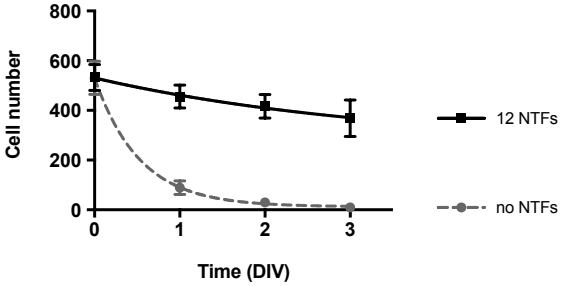

Supplemental Figure S2. Biological activity of neurotrophic factors on motor neuron survival.

A. Full biological activity of all 12 neurotrophic factors (NTFs) was verified by comparing side by side the effects of different commercial batches purchased from Life Technologies (L), Miltenyi (M), R&D Systems/Bio-Techne (R), Sigma (S) and Tebu (T). NTFs were prepared according to the supplier's recommendations and diluted to their reported optimal concentration (Table 4) in chemically defined medium. Motor neurons (MN) were isolated by high speed FACS from mouse lumbar spinal cord, automatically seeded into 96-well cell culture dishes, and cultured in the presence of a single NTF, all 12 NTFs or no NTFs. Analysis of motor neuron cell survival (mean ± sd) at 3 DIV revealed significant biological activity of single NTFs in comparison to no NTFs. NTFs from different suppliers had similar biological activities, except batches of GDNF and LIF. Statistical significance was tested by Kruskal-Wallis test and Tukey post hoc test, n = 6 wells per condition : * $p < 0.01$; ns: not significant.

B. Survival kinetics of lumbar motor neurons (mean ± sd) cultured for up to 3 DIV in the presence or absence of 12 NTFs. Data were fitted by the non-linear least-squares method (GraphPad Prism) using a one phase exponential decay equation.

Supplemental Fig. S3
Schaller et al.

A Plate design

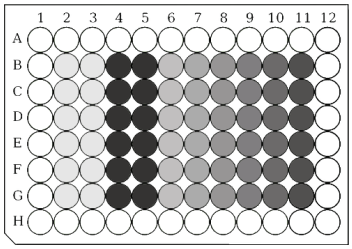

NTFs no all 1 2 3 1+2 1+3 2+3

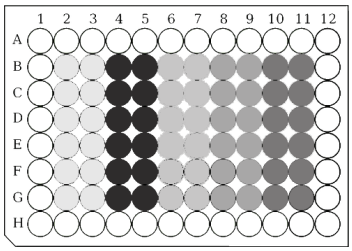

NTFs no all 1 2 1+2

B Flow chart

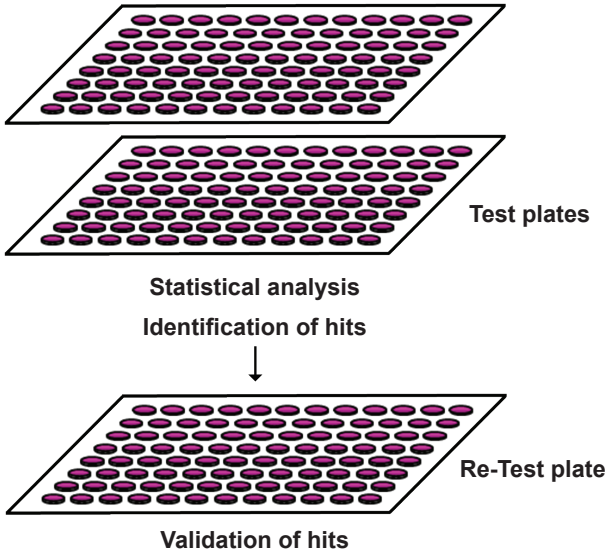

C NTF assay (mean data)

	% Survival NTF	% Survival NTF combination										
GDNF	40,3											
BDNF	25,0	64,4										
HGF	21,8	61,7	50,6									
NTN	21,0	56,9	35,6	33,1								
NT3	12,5	53,9	32,8	19,0	18,1							
ARTN	10,3	49,0	44,6	40,0	16,6	12,2						
LIF	8,0	50,4	30,5	28,7	29,1	27,2	24,3					
IGF1	7,9	46,0	29,3	35,2	37,4	19,2	10,9	20,5				
CNTF	7,8	49,6	34,4	35,9	25,1	21,5	21,7	10,7	10,9			
VEGF	6,7	45,6	37,2	31,0	30,4	9,0	12,6	20,0	12,0	12,0		
PSP	4,8	37,5	35,7	20,8	17,2	18,6	8,6	4,6	11,9	14,9	10,2	
CT1	2,0	35,0	35,3	18,0	24,3	13,2	8,9	10,1	9,1	4,5	5,0	4,5
		40,3	25,0	21,8	21,0	12,5	10,3	8,0	7,9	7,8	6,7	4,8	2,0
		GDNF	BDNF	HGF	NTN	NT3	ARTN	LIF	IGF1	CNTF	VEGF	PSP	CT1

D NTF assay (median data)

	% Survival NTF	% Survival NTF combination										
GDNF	43,0											
BDNF	23,2	58,1										
HGF	20,6	62,2	49,6									
NTN	20,1	56,7	37,2	34,0								
NT3	12,2	52,3	31,1	14,1	17,2							
ARTN	11,7	45,6	41,8	41,3	14,3	11,9						
LIF	7,0	46,3	31,2	31,7	28,4	30,6	24,7					
IGF1	7,0	46,5	29,0	34,6	34,6	19,6	10,7	19,6				
CNTF	6,9	50,3	35,4	37,6	26,6	21,6	25,3	13,3	10,8			
VEGF	5,4	44,5	35,4	31,6	33,8	9,2	10,7	20,4	10,4	12,4		
PSP	4,4	35,9	35,6	21,3	19,1	17,9	10,9	4,2	8,3	12,9	13,7	
CT1	3,7	34,8	35,0	18,0	29,9	13,4	8,1	10,7	10,8	7,4	4,1	4,9
		43,0	23,2	20,6	20,1	12,2	11,7	7,0	7,0	6,9	5,4	4,4	3,7
		GDNF	BDNF	HGF	NTN	NT3	ARTN	LIF	IGF1	CNTF	VEGF	PSP	CT1

E NTF assay (range of data)

	% Survival NTF	% Survival NTF combination										
GDNF	33,6 - 47,6											
BDNF	17,0 - 30,7	55,9 - 61,6										
HGF	12,4 - 30,9	61,6 - 68,6	47,4 - 58,0									
NTN	13,8 - 27,6	51,7 - 60,4	29,0 - 41,9	32,2 - 34,4								
NT3	7,8 - 17,3	50,8 - 56,8	28,2 - 38,4	11,3 - 26,2	14,8 - 21,6							
ARTN	9,0 - 16,1	44,3 - 56,8	39,6 - 51,9	38,9 - 43,1	8,5 - 22,5	7,7 - 12,1						
LIF	3,5 - 10,7	43,6 - 51,9	28,0 - 32,4	28,2 - 35,2	26,3 - 32,6	25,3 - 32,0	23,2 - 26,1					
IGF1	3,8 - 8,9	41,4 - 51,5	28,4 - 29,9	30,1 - 39,9	32,2 - 40,4	17,6 - 24,7	7,4 - 14,0	18,8 - 22,2				
CNTF	1,6 - 11,5	45,6 - 52,4	32,8 - 40,1	30,7 - 43,6	21,4 - 28,2	16,1 - 26,3	24,3 - 26,3	9,4 - 17,1	10,1 - 12,1,			
VEGF	1,7 - 11,8	36,1 - 52,0	27,8 - 43,6	23,0 - 36,8	23,2 - 35,7	8,8 - 10,4	4,6 - 14,5	15,3 - 22,1	10,4 - 15,4	10,3 - 15,9		
PSP	2,1 - 9,3	28,7 - 44,4	24,2 - 40,9	17,8 - 23,3	14,2 - 20,9	12,7 - 22,4	5,8 - 12,6	0,6 - 5,0	7,8 - 17,2	9,1 - 20,1	2,9 - 16,8	
CT1	0,1 - 7,4	31,4 - 41,9	34,9 - 38,4	17,2 - 18,9	26,9 - 34,7	12,4 - 15,2	2,3 - 14,4	7,9 - 13,4	4,8 - 13,5	1,3 - 8,2	-3,3-15,5	4,0 - 5,0
		33,6 - 47,6	17,0 - 30,7	12,4 - 30,9	13,8 - 27,6	7,8 - 17,3	9,0 - 16,1	3,5 - 10,7	3,8 - 8,9	2,6 - 11,5	1,7 - 11,8	2,1 - 9,3	0,1 - 7,4
		GDNF	BDNF	HGF	NTN	NT3	ARTN	LIF	IGF1	CNTF	VEGF	PSP	CT1

Supplemental Figure S3. Screening NTF combinations.

A. Design of test and re-test plates. 96-well test plates (upper panel) contain rows with negative controls (culture medium only), positive controls (all 12 NTFs in culture medium), three individual NTFs (1, 2, 3) and all three pairwise NTF combinations (1+2, 1+3, 2+3). Re-test plates (lower panel) are used to confirm the effects of two NTFs in combination. Plates are prepared prior to FACS by manual pipetting of culture medium (135 µl) and addition of NTFs or NTF combinations (15 µl) at 10-fold final concentration in culture medium. Wells on the edges are filled with water.

B. Flow chart for data analysis and processing, ref. (1). Statistical differences between conditions on each plate are tested by Kruskal Wallis test and Dunn's post hoc test.

C. NTF assay showing mean values of motor neuron survival. Survival data are expressed relative to no NTFs (set 0%) and all 12 NTFs (set 100%).

D. NTF assay showing median values of motor neuron survival.

E. NTF assay showing range of data (25% - 75% percentiles).

Supplemental Fig. S4
Schaller et al.

A Marker gene expression in motor neuron subsets

			Fold change LMC/PGC vs MMC						
Gene	**Synonyme**	**GSM**	**mean**	**sd**	**#1**	**#2**	**#3**	**p-value**	**MN marker**
Pou3f1	Oct6, Scip	GSMG0027043	-2,78	0,274287	-2,62	-2,63	-3,1	9.41E-4	MMC
Lhx3		GSMG0022555	-9,73	2,046485	-9,22	-8,21	-12,15	2.95E-4	MMC
Lhx4		GSMG0002258	-4,89	0,228108	-8,21	-8,61	-8,22	2.71E-3	MMC
Aldh1a2	Raldh2	GSMG0039772	24,25	5,461734	18,6	26,3	29,16	1.1E-3	LMC
Lhx1		GSMG0007133	5,6	0,653682	6,31	5,01	5,54	1.2E-3	LMC
Foxp1	FoxP1	GSMG0033453	2,18	0,542248	2,82	2,06	1,77	3.67E-2	LMC/PGC
Nos1	nNos	GSMG0029706	3,26	0,40129	3,5	3,51	2,81	4.51E-3	PGC
Hnf6	Onecut1	GSMG0039805	3,68	0,633798	4,31	3,8	3,05	7.56E-4	PGC
Smad1		GSMG0038636	1,36	0,091652	1,34	1,46	1,28	3.11E-3	PGC

B Global gene expression analysis in FACS-isolated motor neuron subsets

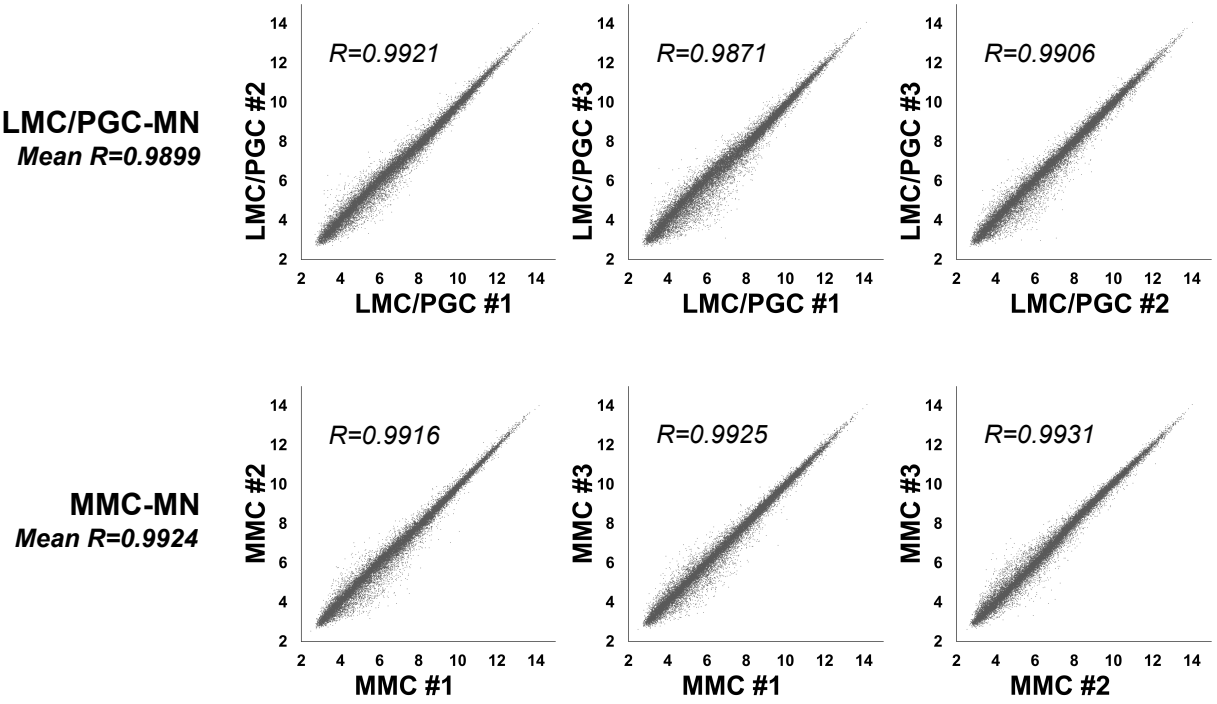

Supplemental Figure S4. Gene expression profiles of LMC/PGC motor neurons and MMC motor neurons on microarrays.

A. Gene expression profile of marker genes in LMC/PGC-MN and MMC-MN. Fold changes (mean, sd, sample pairs #1, #2, #3) and p-values by student's t-test are indicated.

B. Global gene expression analysis in FACS-isolated motor neuron subsets. Scatter plots and correlation coefficients of gene expression (R) between independent biological replicates #1, #2 and #3 of LMC/PGC-MN and MMC-MN show high standardization. Expression values are on log2 scale.

Supplemental Fig. S5
Schaller et al.

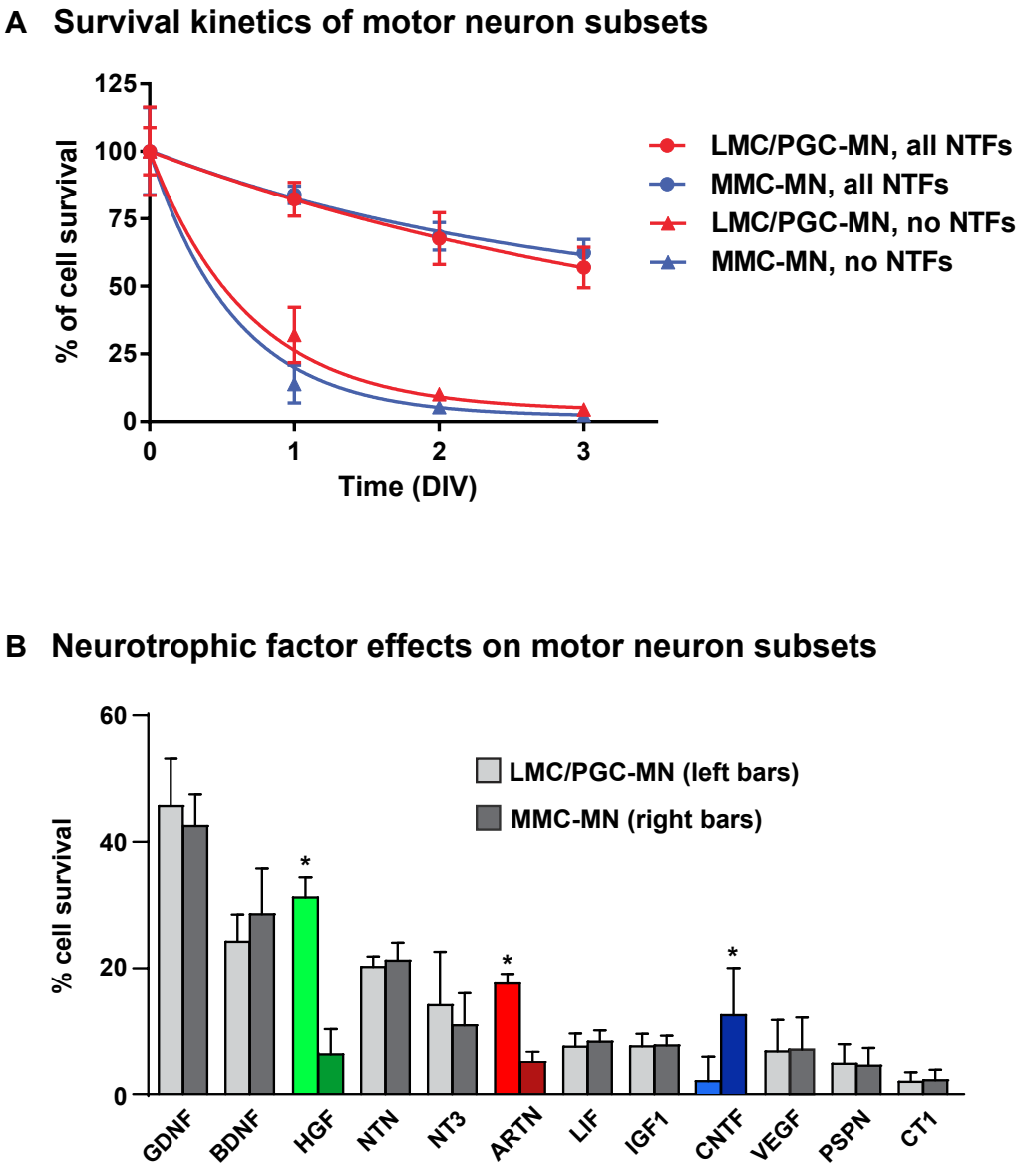

Supplemental Figure S5. Gene expression profile and NTF survival responses of LMC/PGC and MMC motor neurons.

a. Similar survival kinetics (mean ± sd) of FACS-isolated LMC/PGC-MN and MMC-MN from 0 to 3 DIV. There are no significant survival differences between LMC/PGC-MN and MMC-MN cultured in the presence or absence of NTFs. The kinetic data were fitted by a non-linear least-squares method (GraphPad Prism) using a one phase exponential decay equation.

b. Similar survival responses of LMC/PGC-MN (light shaded bars) and MMC-MN (dark shaded bars) to the neurotrophic factors CNTF, BDNF, NTN, LIF, IGF1, VEGF, PSPN and CT1. Distinct survival responses are seen for HGF, ARTN and CNTF (mean ± sd, * $p < 0.05$, Mann & Whitney test). Survival values are expressed relative to the value obtained in the presence of all NTFs (100 %) or no NTF (0 %).

Supplemental Fig. S6
Schaller et al.

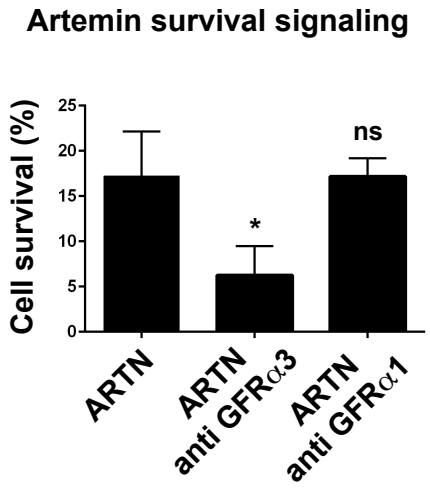

Supplemental Figure S6. GFRα3-mediated Artemin survival signaling.
Cell survival of motor neurons cultured in the presence of Artemin (ARTN) is significantly inhibited by pre-incubation with antibodies against the extracellular domain of GFRα3 (2 μg/ml, 1 h) but not with antibodies against GFRα1 (10 μg/ml, 1 h). *, p = 3.28 E-7 by student's t-test; ns: not significant.

Supplemental Materials and Methods

Reagents. Antibodies, neurotrophic factors, pharmacological inhibitors and antisense probes are listed in **Tables 1-6**. Other reagents (references, suppliers) were as follows: DIG-labeling kits, yeast RNA and RNase (Roche), bovine serum albumin (BSA), DNase I (DN25), trypsin, bovine hemoglobin (H2625-25G), poly-DL-ornithin (P8638) (Sigma), L15 (11415-064), B27 (17504-044), Neurobasal without riboflavin (041-96399M) (Thermofisher), laminin (354232, Corning), calcein (FP-855422, Interchim), Triton X-100 (Euromedex), Facsflow (342003), Facsrinse (340346) (Becton Dickinson), 24-well plates (142475, Nunc), 96-well plates (655090, Greiner or 353219, Falcon) and 384-well plates (781091, Greiner).

Gene expression profiling. FACS-isolated motor neurons were collected at a minimum yield of 60.000 cells per subtype in each of three replicate experiments. RIN values were between 8.1 and 9.5 (mean 8.9). Gene expression profiling was performed using Mouse Exon 1.0 ST arrays (Affymetrix, Hygh Wycombe, UK) according to the supplier's recommendations. Raw data were controlled with Expression console (Affymetrix) and analyzed by GenoSplice using EASANA software and FAST DB annotations (2).

Immunoblot analyses. FACS-isolated motor neurons were collected in ice-cold Laemmli buffer, protein extracts corresponding to 20.000 motor neurons separated by SDS-PAGE and blotted on membranes. Membranes were reacted with antibodies (**Table 3**) and revealed with a ChemiDoc XRS+ imager (Biorad).

Immunohistochemistry. Transverse sections of E12 mouse embryos were incubated with primary antibodies and biotinylated or fluorochrome-conjugated secondary reagents (**Table 1**). Slides were mounted with Vectashield/DAPI and images acquired with an inverted Leica DMI 4000B microscope or a Zeiss LSM510 confocal microscope.

Retrograde labeling. Urogenital organs including bladder (3) of E12 Hb9:GFP embryos were identified using a fluorescence dissection microscope (Leica FZ III). Injection of Dextrans conjugated to AlexaFluor or Tetramethylrhodamine were performed using a microcapillary. Embryos were incubated for 3 to 4 hours at 30°C in Hibernate medium containing 1% penicillin-streptomycin under continuous CO_2/O_2 bubbling. Embryos were then either processed for immunohistochemistry or their spinal cords were dissected out. Preparation of single cell suspensions and flow cytometry analysis were done as described above.

Signaling studies. Pharmacological inhibitors are listed in **Table 5**. The monovalent antibody against mouse c-Met (OA-118) was designed, produced and tested for its biological activity as described (4). Unless otherwise stated, FACS-isolated motor neurons were pre-incubated with the inhibitors for 1 h before NTF addition. Optimal concentrations of each inhibitor were empirically determined.

Whole mount labelings. E12 spinal cords were reacted with digoxigenin (DIG)-labelled RNA probes (**Table 6**) or anti-GFRα3 antibodies. In situ hybridization and in situ immunohistochemistry were performed by standard techniques (5) and images acquired with a Leica MZ 12 microscope.

Tables

Table 1. Antibodies used in immunohistochemistry

Primary Antibodies	Dilution	Supplier	Reference
Choline Acetyl Transferase (goat)	1:100	Chemicon	Ab144P
Engrailed 1 (EN1) (mouse)	1:20	DSHB	4G11
CHX10 (sheep)	1:50	Exalpha	X1179P
GFRα3 (goat)	1:500	R&D Systems	AF2645
Neurofilament M (rabbit)	1:1000	Merck Millipore	AB1987
Neurofilament H non phosphorylated SMI32 (mouse)	1:500	Sternberger	SMI-32R
nNOS C-ter (rabbit)	1:300	Immunostar	24287
Fox P1 (rabbit)	1:500	Abcam	ab16645

Secondary antibodies and tracers	Dilution	Supplier	Reference
anti-goat Biotin (donkey)	1:500	Jackson Lab.	705-066-147
Streptavidin Alexa Fluor 594	1:500	Invitrogen	S32356
anti-rabbit Cy5 (donkey)	1:300	Jackson Lab.	711-175-152
anti-mouse Cy5 (donkey)	1:200	Jackson Lab.	711-175-151
anti-sheep Cy3 (donkey)	1:200	Jackson Lab.	713-165-147
Dextran Alexa 647	50 mg/ml	Invitrogen	D22914
Dextran Tetramethylrodamine	50 mg/ml	Invitrogen	D1817

Table 2. Antibodies used in flow cytometry

Primary Antibodies	Dilution	Supplier	Reference
Hb9 (mouse)	1:100	DSHB	81.5C10
Islet-1 / Islet-2 (mouse)	1:100	DSHB	40.2D6 / 39.4D5
Lhx 1/2 (mouse)	1:100	DSHB	4F2
Lhx 3 (mouse)	1:100	DSHB	67.4E12
Foxp1 (mouse)	1:2000	Abcam	ab32010
Oct6 (mouse)	1:2000	S. Driegen	(6)

Secondary Antibodies	Dilution	Supplier	Reference
anti-mouse IgG Alexa Fluor 568 (donkey)	1:1000	Invitrogen	A10037
anti-rabbit IgG Alexa Fluor 568 (donkey)	1:1000	Invitrogen	A10042
anti-mouse IgG Alexa Fluor 633 (goat)	1:2000	Invitrogen	A21052
anti-rabbit IgG Alexa Fluor 633 (goat)	1:2000	Invitrogen	A21070
anti-sheep IgG (donkey)	1:2000	Invitrogen	A21099

Table 3. Antibodies used in immunoblots

Primary Antibodies	Dilution	Supplier	Reference
c-Met (mouse)	1:1000	Cell Signaling	3127
c-Ret (C-19) (rabbit)	1:200	Santa Cruz	sc-167

GFRα3 (goat)	1:100	R&D Systems	AF2645
Gp130 (C-20) (rabbit)	1:100	Santa Cruz	sc-655
H3 (mouse)	1:200	Merck Millipore	05-499
LIF Rβ (H-220) (rabbit)	1:100	Santa Cruz	sc-20752
Syndecan-3 (rabbit)	1:500	Abcam	Ab63932

Secondary Antibodies	**Dilution**	**Supplier**	**Reference**
HRP - anti-rabbit (goat)	1:40.000	Invitrogen	62-6120
HRP - anti-goat (donkey)	1:40.000	Jackson Lab.	705-036-147
HRP - anti-mouse (goat)	1:40.000	Jackson Lab.	115-036-062
HRP - anti-rabbit (goat)	1:40.000	Jackson Lab.	111-036-045
HRP - anti-rabbit (goat)	1:40.000	Jackson Lab.	111-035-144

Table 4. Neurotrophic factors

Neurotrophic factor	**Final concentration (ng/ml)**	**Supplier**	**Reference**
ARTN	10	R&D Systems	1085-AR
BDNF	1	R&D Systems	248-BD
CNTF	10	R&D Systems	557-NT
CT1	10	R&D Systems	438-CT
GDNF	1	Life Technologies	PHC7041
HGF	2	R&D Systems	2207-HG
IGF1	100	R&D Systems	791-MG
LIF	10	Life Technologies	PMC4054
NT3	10	R&D Systems	267-N3
NTN	10	R&D Systems	477-MN
PSPN	10	R&D Systems	2479-PS
VEGF	100	R&D Systems	493-MV

Table 5. Pharmacological inhibitors

Inhibitor	**Conc. / Dilution**	**Supplier**	**Reference**
EMD 1204831	100 nM	Merck	(7)
OA-118	5 μg/ml	Genentech	(4)
Heparinase III	1:10.000	R&D Systems	6145-GH
PI-PLC	2 μg/ml	Sigma-Aldrich	P8804
anti-GFRα1	10 μg/ml	R&D Systems	AF560
anti-GFRα3	2 μg/ml	R&D Systems	AF2645

Table 6. Antisense probes used for in situ hybridization

Probe	Restriction Enzyme/ RNA Polymerase	Origin	Reference
Met 5'	BamHI/T3	Y. Yamamoto	(8)
Met 3'	NotI/T3	Y. Yamamoto	(8)
Ret	NotI/T7	V. Pachnis	(9)
Gfra3	BamHI/T3	P. Ernfors	(10)
Hb9	EcoRV/T7	J. Livet	unpublished
Lifrb	EcoRI/T3	H. Nishimune	(11)
Raldh2	XbaI/T7	T. Jessell	(12)

Supplemental References

1. Malo N, Hanley JA, Cerquozzi S, Pelletier J, & Nadon R (2006) Statistical practice in high throughput screening data analysis. *Nature Biotechnology* 24(2):167-175.

2. de la Grange P, Dutertre M, Correa M, & Auboeuf D (2007) A new advance in alternative splicing databases: from catalogue to detailed analysis of regulation of expression and function of human alternative splicing variants. *BMC Bioinformatics* 8:180.

3. Islam SS, et al. (2013) Spatio-temporal distribution of Smads and role of Smads/TGF-beta/BMP-4 in the regulation of mouse bladder organogenesis. PLoS One 8(4):e61340.

4. Merchant M, et al. (2013) Monovalent antibody design and mechanism of action of onartuzumab, a MET antagonist with anti-tumor activity as a therapeutic agent. *Proc Natl Acad Sci U S A* 110(32):E2987-2996.

5. Haase G, et al. (2002) GDNF acts through PEA3 to regulate cell body positioning and muscle innervation of specific motor neuron pools. *Neuron* 35(5):893-905.

6. Jagalur NB, et al. (2011) Functional dissection of the Oct6 Schwann cell enhancer reveals an essential role for dimeric Sox10 binding. *Journal of Neuroscience* 31(23):8585-8594.

7. Bladt F, et al. (2013) EMD 1213063 and EMD 1204831 constitute a new class of potent and highly selective c-Met inhibitors. *Clin Cancer Res* 19:2941-2951.

8. Yamamoto Y, et al. (1997) Hepatocyte growth factor (HGF/SF) is a muscle-derived survival factor for a subpopulation of embryonic motoneurons. *Development* 124(15):2903-2913.

9. Pachnis V, Mankoo B, & Costantini F (1993) Expression of the c-ret proto-oncogene during mouse embryogenesis. *Development* 119(4):1005-1017.

10. Naveilhan P, et al. (1998) Expression and regulation of GFRalpha3, a glial cell line-derived neurotrophic factor family receptor. *Proc Natl Acad Sci U S A* 95(3):1295-1300.

11. Nishimune H, et al. (2000) Reg-2 is a motoneuron neurotrophic factor and a signalling intermediate in the CNTF survival pathway. *Nat Cell Biol* 2(12):906-914.

12. Sockanathan S, Perlmann T, & Jessell TM (2003) Retinoid receptor signaling in postmitotic motor neurons regulates rostrocaudal positional identity and axonal projection pattern. *Neuron* 40(1):97-111.